

SCIENTIFIC REPORTS

OPEN

Hypervalent Iodine with Linear Chain at High Pressure

Shubo Wei¹, Jianyun Wang¹, Shiyu Deng², Shoutao Zhang¹ & Quan Li^{1,2}

Received: 27 May 2015

Accepted: 28 August 2015

Published: 24 September 2015

Iodine is an element of fascinating chemical complexity, and numerous hypervalent iodine compounds reveal vital value of applications in organic synthesis. Investigation of the synthesis and application of new type of hypervalent iodine compound has extremely significant meaning. Here, the formation of CsI_n ($n > 1$) compounds is predicted up to 200 GPa using an effective algorithm. The current results show that CsI_3 with space group of $Pm-3n$ is thermodynamically stable under high pressure. Hypervalence phenomenon of iodine atoms in $Pm-3n$ CsI_3 with endless linear chain type structure appears under high pressure, which is in sharp contrast to the conventional understanding. Our study further reveals that $Pm-3n$ CsI_3 is a metallic phase with several energy bands crossing Fermi-surface, and the pressure creates a peculiar reverse electron donation from iodine to cesium. The electron-phonon coupling calculations have proposed superconductive potential of the metallic $Pm-3n$ CsI_3 at 10 GPa which is much lower than that of CsI (180 GPa). Our findings represent a significant step toward the understanding of the behavior of iodine compounds at extreme conditions.

Iodine compounds have always been the subject of extensive studies because of their significant properties such as conduction characteristic^{1,2}, optical property³, catalytic performance^{4,5} and medical application⁶, etc. For instance, cesium iodide (CsI) is one of the simplest and most representative ionic solids, and extensive theoretical and experimental studies have been carried out^{7–15}. CsI exhibits variety of interesting phenomena such as pressure involved metallization and superconductivity under high pressure^{12–14}. In addition, organic molecules bearing hypervalent iodine moieties have been transformed from laboratory curiosities to useful and routinely employed reagents in organic synthesis^{16–21}. Comparing with the relatively and easily synthesized organic complexity, the synthesis of inorganic hypervalent iodine compounds with attractive properties and its corresponding structures have been a long-standing puzzle. For I_3^- ion, its linear geometric structure was determined for the first time in 1935 by Mooney, who carried out X-ray analysis on ammonium triiodide²². The I_3^- anion belongs to the type of compounds known as hypervalent, which violate the Lewis octet rule²³. Due to the representative hypervalence property of I_3^- ion, it is of great consideration for further study of CsI_n ($n > 1$) compounds to explore the possibility of forming hypervalent CsI_n with interesting properties or structures. Previous experimental works show that crystal CsI_3 and CsI_4 can be synthesized at ambient pressure^{24–27}. Subsequently, experimental XRD measurement proposed that the crystal information of CsI_3 and CsI_4 were orthorhombic $Pmnb$ and monoclinic $P2_1/a$ symmetry, respectively^{28–30}. W. Zhang *et al.* did an excellent work for Na_xCl system by combining theoretical predictions and diamond anvil cell experiments³¹. They reported that Na_3Cl , Na_2Cl , Na_3Cl_2 , NaCl_3 and NaCl_7 are theoretically stable and have unusual bonding and electronic properties at high pressure³¹. Na-Cl and Cs-I system are clearly analogous as typical ionic solids and they may adopt the same structures. Currently, the synthesis or the full high-pressure structural information of CsI_n are still far from being clear and established. These structural uncertainties have impeded in-depth understanding and further exploration of phenomena of CsI_n might under compression.

Here, we present systematic structure searches to establish the thermodynamically stable structures of CsI_n ($n = 2 - 5$) up to 200 GPa using the developed CALYPSO (Crystal structure ANALysis by Particle

¹State Key Laboratory of Superhard Materials, Jilin University, Changchun 130012, China. ²College of Materials Science and Engineering, Jilin University, Changchun 130012, China. Correspondence and requests for materials should be addressed to Q.L. (email: liquan777@jlu.edu.cn)

Swarm Optimization) method^{32–35}, which has been successfully used in numerous predictions regarding compounds and structures over the past few years^{36–46}. Our work shows that CsI₃ has the simple *Pmnb* structure at ambient pressure and undergoes a complicated transition to high symmetric cubic *Pm-3n* phase at high pressure. The current *Pm-3n* phase of CsI₃ is a metal phase, and the pressures create a peculiar reverse electron donation from iodine to cesium. In addition, the iodine atoms of *Pm-3n* phase forming into several completely linear chains show an attractive hypervalence phenomenon, which cannot be simply explained by traditional three-center-four-electron (3c-4e) scheme^{47–49}. This work presents significant concerning on the synthesis and the fundamental structural properties of the simplest and most representative polyiodide materials with implications for an entire family of similar materials.

Calculation Methods

To obtain stable structures for CsI_{*n*}, we carried out a structural search using a global minimization of free energy surfaces based on the CALYPSO methodology^{32–35} and the first-principles calculations. The remarkable feature of this methodology is the capability of predicting the stable structure with only the knowledge of the chemical composition at given external conditions (for example, pressure). The underlying *ab initio* structural relaxations, electron localization function (ELF) and electronic band structure calculations were performed within the framework of density functional theory (DFT) as implemented using by VASP (Vienna *ab initio* simulation package) code⁵⁰. The generalized gradient approximation (GGA) within the framework of Perdew–Burke–Ernzerhof (PBE)⁵¹ was used for the exchange–correlation functional. And the projector augmented wave method (PAW)⁵² has been adopted, with 5s²5p⁶6s¹ and 5s²5p⁵ treated as valence electrons for cesium and iodine, respectively. The cutoff energy for the expansion of the wavefunction into plane waves was set at 400 eV and fine Monkhorst–Pack (MP) *k* meshes of 0.025 Å^{−1} have been chosen to ensure that all the enthalpy calculations are well converged. The phonon calculations have been carried out by using a supercell approach as implemented in the Phonopy code⁵³. This method uses the forces obtained by the Hellmann–Feynman theorem calculated from the optimized 3 × 3 × 3 supercell. The Bader’s quantum theory of atoms in molecules (QTAIM) analysis⁵⁴ was used for charge calculation.

Electron-phonon coupling (EPC) calculations have been performed using the pseudo-potential plane-wave method and density-functional perturbation theory^{55,56} as implemented in the Quantum-ESPRESSO package⁵⁷. EPC calculation has been performed on 4 × 4 × 4 MP *q* meshes in the first Brillouin zone with a kinetic energy cutoff of 60 Ry. 16 × 16 × 16 MP *k* meshes are chosen to ensure *k*-point sampling convergence with Gaussians of 0.025 Ry, which approximates the zero-width limit in this calculation.

Results and Discussions

The high-pressure synthesis and structural information of CsI_{*n*}. Structural predictions for CsI_{*n*} (*n* = 2 – 5) have been performed with CALYPSO methodology^{32–35} using simulation sizes with 1–4 formula per primitive cell under a series of pressure points (0, 50, 100, 150 and 200 GPa). The enthalpy of formation per atom is calculated using the following formula:

$$\Delta H_f(\text{CsI}_n) = [H(\text{CsI}_n) - H(\text{CsI}) - (n - 1)H(\text{I}_2)/2]/(n + 1)$$

where ΔH_f is the enthalpy of formation per atom and *H* is the calculated enthalpy per chemical unit for each compound.

From the convex hull shown in Fig. 1a (solid lines), only CsI₃ with space group of *Pm-3n* is thermodynamically stable under high pressure. However, previous experimental work shows that CsI₄ can be synthesized at ambient pressure, and a *P2₁/a* phase with 4 formulas per primitive cell has been proposed by X-ray analysis²⁹. The currently predicted *Pnma* phase is energetically much superior to the monoclinic *P2₁/a* structure, while the formation enthalpy of *Pnma* is positive value and thus does not support its thermodynamic stability. We note that the experimentally synthesized CsI₄ was heated in a closed vessel at 90 °C, and was then cooled slowly to 25 °C²⁹. Therefore, the *P2₁/a* CsI₄ structure is a metastable phase. CsI₃ is stable at ambient pressure and adopts an orthorhombic lattice with *Pmnb* symmetry (Fig. 2a). The optimized lattice parameter of *Pmnb* phase at 0 GPa is *a* = 7.2366 Å, *b* = 11.2631 Å and *c* = 10.4905 Å. At 0 GPa, this actually Cs⁺[I₃][−] phase contains linear type I₃[−] ions with two I–I bonds length of 2.901 and 3.019 Å, which are similar to the experimental data of 2.820 and 3.100 Å²⁸, respectively. Such typical hypervalent iodine moiety of orthorhombic *Pmnb* structure can be conventionally explained by traditional theory. For I₃[−] ion of *Pmnb* phase, the central iodine atom shares two electrons with two adjacent iodine atoms by forming one 3c-4e bond, and meanwhile it gets one electron from cesium atom to keep the other two iodine atoms following Lewis octet rule²³. On the other hand, Pauling⁵⁸ and Cartmell⁵⁹ interpreted the hypervalence phenomenon of this ion in terms of the trigonal-bipyramidal orbitals of the central atom (*sp³d* hybridization). The central iodine atom has 10 electrons in valence shell which supports the conventional hypervalence phenomenon. The *Pmnb* structure remains stable up to 7.8 GPa, where undergoes a complicated first-order phase transition to cubic *Pm-3n* structure with volume collapse of 7.19% (Fig. 1b). The optimized lattice parameters of *Pm-3n* phase at 10 GPa is *a* = 6.2865 Å. Atoms occupy the Wyckoff 2*a* (0, 0, 0) for cesium and 6*d* (0, 0.5, 0.75) for iodine. Surprisingly, the

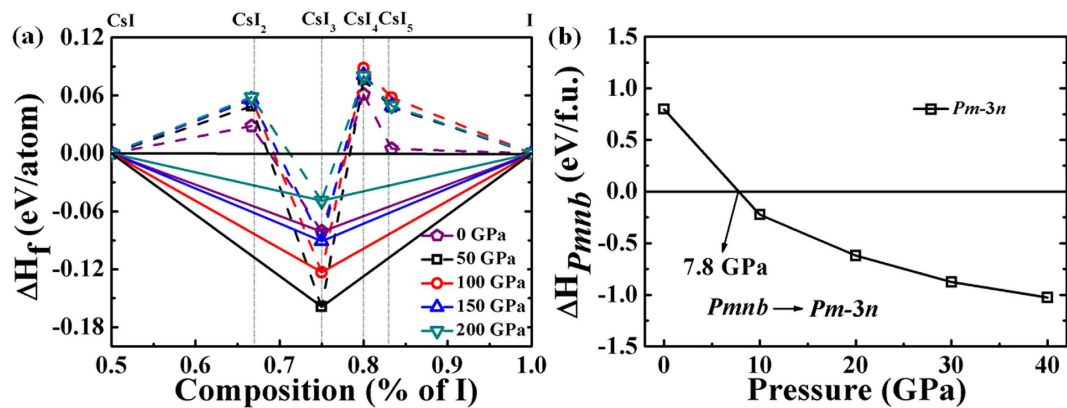


Figure 1. Enthalpy calculations of CsI_n . (a) Enthalpies of formation of CsI_n under a range of pressures. Dotted lines connect data points, and solid lines denote the convex hull. (b) Enthalpy (related to the $Pmnb$ phase) of $Pm-3n$ structure for CsI_3 as a function of pressures.

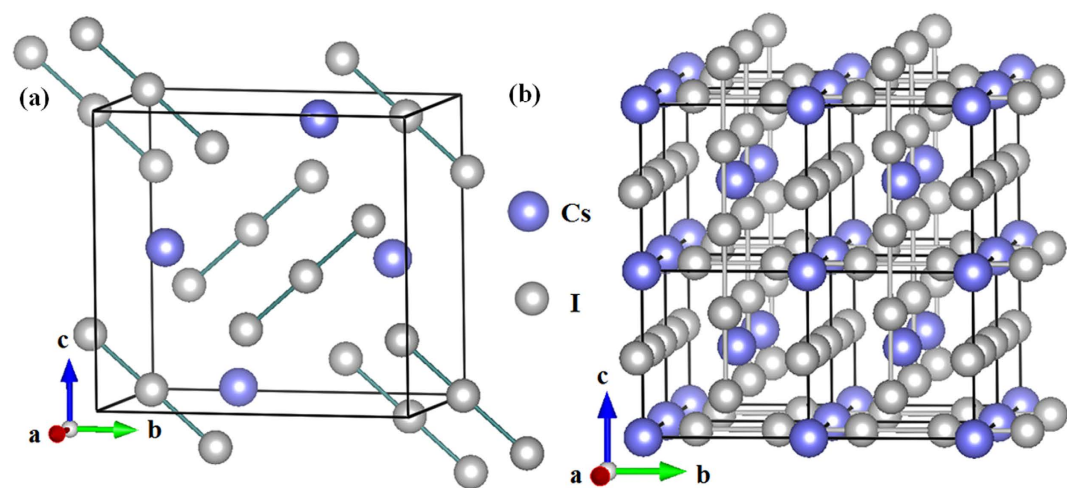


Figure 2. Crystal structures of CsI_3 . (a) CsI_3 at 0 GPa with actual formula of $\text{Cs}^+[\text{I}_3]^-$. (b) CsI_3 at 10 GPa in a cubic $Pm-3n$ structure.

enthalpies of $Pm-3n$ phase at least up to 200 GPa from convex hull (Fig. 1a) show that $Pm-3n$ phase tends to decompose as the increasing pressure.

Comparing with orthorhombic $Pmnb$ structure, a striking feature of this modification is that all the iodine atoms form endless linear chains (Fig. 2b). And these endless chains just locate on the surface of the $Pm-3m$ Cs lattice. The lattice dynamics calculations with no imaginary phonon frequencies support the dynamic stability of $Pm-3n$ structure over the pressure range studied here (Fig. 3a). Remarkly, the endless chain structure has rarely been found in inorganic compounds before. One previous work shows that the B atoms of Li_2B can form kinked chains along the c axis under high pressure³⁸. However, such kinked chains of B is clearly different from iodine chains which are thoroughly linear without any tortuosity. The similar crystal structures with $Pnma$ and $Pm-3n$ space groups have been reported for NaCl_3 ³¹. NaCl_3 is stable in the $Pnma$ containing almost linear asymmetric Cl_3 groups at 20 to 48 GPa, and then transforms into a metallic $Pm-3n$ structure. NaCl_3 and CsI_3 are clearly analogous compounds and even adopt the same structures, and Cl-Cl bonds in $Pm-3n$ NaCl_3 similar with our predicted I-I bonds by forming extended monatomic chains running along the three mutually perpendicular axes³¹. In addition, the Cs-I bond length in CsI_3 is close to that in CsI as pressures change, indicating the forming of Cs-I ionic bond (Fig. 3b). And the I-I bond length in CsI_3 is 2.764 Å at 60 GPa, significantly shorter than the shortest I-I distances of 3.021 Å in solid I_2 (Fig. 3b), showing a stronger bonding character. The ELF of CsI_3 at 150 GPa shows that the strongest electron localization area are located between iodine and iodine atoms (Fig. 3c), suggesting covalent bond forms between the iodine atoms. As we well know, pressure-induced molecular dissociation of solid I_2 has been reported from theoretical or experimental studies, but iodine in $Pm-3n$ phase can held together by strong chemical bonds at least until 200 GPa. We have calculated the charges using Bader's quantum theory of atoms in molecules (QTAIM) analysis⁵⁴ for

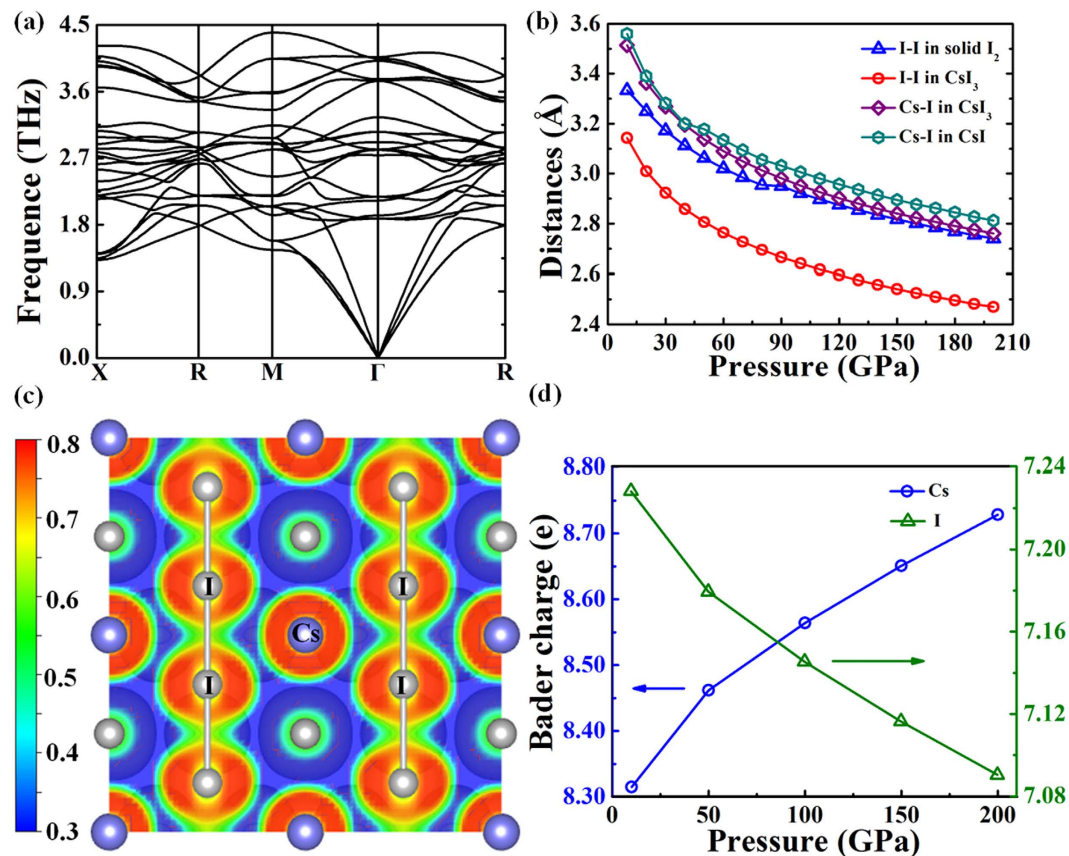


Figure 3. The lattice dynamics and bonding behavior analysis of $Pm-3n$ CsI_3 . (a) Calculated phonon spectrum of $Pm-3n$ CsI_3 at 10 GPa. (b) Interatomic distances (between atoms shown in the structure directly underneath) in I_2 , CsI_3 and CsI as a function of external pressure. (c) ELF of CsI_3 at 150 GPa. (d) Calculated Bader charge of cesium and iodine in CsI_3 as a function of external pressure.

CsI_3 at high pressure. From Fig. 3d, the electrons devoted from cesium to iodine are gradually reduced as the increasing pressure, indicating a peculiar reverse electron donation from iodine to cesium, and thus naturally gives rise to suppress the strength of Cs–I bonds, which is responsible for tendency of the decomposition at higher pressure. Each iodine atom of CsI_3 gets two shared electrons from the nearest-neighbor iodine and averagely 0.3 electrons from cesium atom, and frankly the valence shell of iodine has 9.3 electrons with hypervalence character. Generally, several hypervalent compounds such as hypervalent P, S, I and Xe in PCl_5 , SF_6 , IF_7 and XeF_4 always have integral electrons in valence shell of 10, 12, 14 and 12, respectively⁶⁰. For conventional hypervalent iodine compounds, only one central atom possesses hypervalence property which being surrounded by other several ligands. While in the current ionic CsI_3 compound, all the iodine atoms possess such character, which broadens conventional understanding of hypervalent iodine. Therefore, high pressure induces the attractive hypervalent phenomenon in CsI_3 iodine with specific endless linear chain structure.

At ambient pressure, the prototypical ionic crystal of CsI_3 is an insulator. Interestingly, CsI_3 becomes metallic after the first-order phase transition at 7.8 GPa. The calculated electronic band structures of $Pm-3n$ phase at 10 GPa show it is metallic with several bands crossing Fermi level (Fig. 4a). Pressure induces CsI_3 to exhibit increasingly shorter interatomic distances, which is accompanied by an increase in the bandwidth, especially those near the Fermi-surface, thus leading to the $5p$ bands of iodine expand along conductive band direction (Fig. 4b). Furthermore, the calculated projected density of states (PDOS) of CsI_3 show that the $5d$ states of Cs have more electronic occupation as the pressure increasing (Fig. 4c,d).

It should be mentioned that the superconducting behaviors in CsI have been extensively explored through experimental measurement and theoretical calculations^{12–14}. It is suggested that the formation of several electrons and hole Fermi-surface pockets in CsI is due to a dramatic increase of the electron donation from I^- to Cs^+ , thus leading to more electrons to be involved in the electron-phonon coupling which is responsible for superconductivity and the larger EPC potential, thereby contributing to the increase in T_C ¹². Therefore, it is intriguing to determine whether $Pm-3n$ CsI_3 will possess superconducting property under high pressure.

Figure 5 shows the phonon density of states (PHDOS) and Eliashberg spectral function $\alpha^2F(\omega)$ ⁶¹ for $Pm-3n$ CsI_3 at 10 GPa. It is found that $\alpha^2F(\omega)$ contains two parts of which the low and high frequency

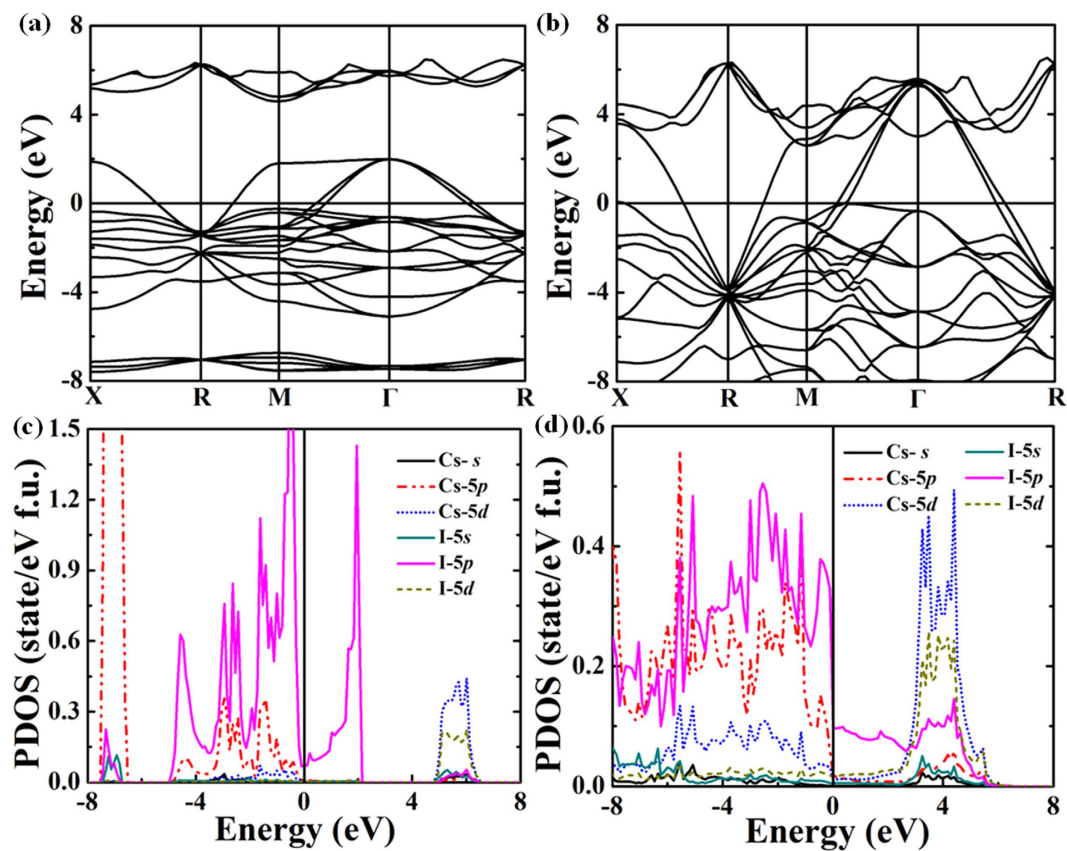


Figure 4. The electronic property analysis of *Pm-3n* CsI₃. Calculated electronic band plot along high-symmetry directions of *Pm-3n* CsI₃ at 10 GPa (a) and 150 GPa (b). Electronic density of states for *Pm-3n* CsI₃ at 10 GPa (c) and 150 GPa (d).

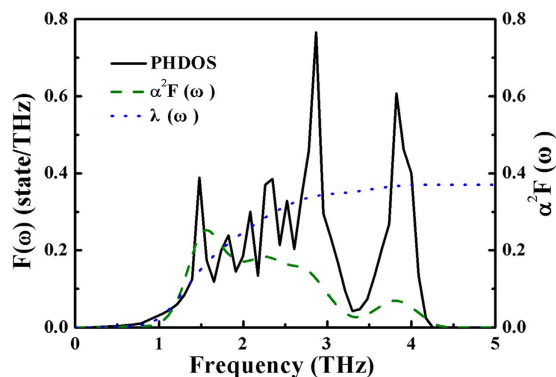


Figure 5. The electron-phonon coupling calculations of *Pm-3n* CsI₃. The calculated phonon density of states (solid line), Eliashberg spectral function $\alpha^2F(\omega)$ (dashed line), and the electron-phonon integral (dotted line) of *Pm-3n* CsI₃ at 10 GPa.

area are localized within a narrow vibrational region of 0.8–3.4 THz and 3.4–4.2 THz, respectively. The integrated EPC λ of low frequency $\alpha^2F(\omega)$ are 0.353 constituting 95.66% of the total λ 0.369, and the other EPC λ in high frequency area is 0.016 accounts 4.34% of total λ . With increasing pressure to 150 GPa, λ was reduced to be 0.074. The superconducting critical temperature T_C can be estimated from the Allen-Dynes modified McMillan equation⁶² $T_C = \frac{\omega_{\log}}{1.2} \exp\left[-\frac{1.04(1+\lambda)}{\lambda - \mu^*(1+0.62\lambda)}\right]$, where ω_{\log} is the logarithmic average frequency calculated directly from the phonon spectrum and μ^* is the Coulomb pseudopotential. ω_{\log} is obtained to be 97.33 K at 10 GPa and 322.96 K at 150 GPa. Using a μ^* of 0.1, the estimated T_C is 0.15 K at 10 GPa but it disappears at 150 GPa. It is noteworthy that the estimated T_C in

CsI₃ is noticeably larger than the value in CsI of 0.03 K, and the pressure is significantly lower than that of CsI (180 GPa).

Conclusions

In summary, we have systematically investigated compounds CsI_n up to 200 GPa using an effective CALYPSO algorithm. Strikingly, CsI₃ with space group of *Pm-3n* is thermodynamic stability under high pressure. Within the cubic *Pm-3n* CsI₃ phase, iodine atoms arranging into several endless linear chains show an attractive hypervalence phenomenon under high pressure, which is in sharp contrast to the conventional understanding. We further discovered that *Pm-3n* CsI₃ is a metallic phase with several energy bands crossing Fermi-surface, and the pressure creates a peculiar reverse electron donation from iodine to cesium. The electron-phonon coupling calculations have proposed superconductive potential of the metallic *Pm-3n* CsI₃ at 10 GPa, which are analogous to the known CsI¹². This work has wide implications for other inorganic compounds that likely harbor similar high-pressure behavior, and the significance for synthetic chemistry is highlighted.

References

- Liang, C. C. Conduction Characteristics of the Lithium Iodide-Aluminum Oxide Solid Electrolytes. *J. Electrochem. Soc.* **120**, 1289–1292 (1973).
- Bradley, J. N. & Greene, P. D. Potassium iodide+silver iodide phase diagram. High ionic conductivity of KAg₃I₅. *Trans. Faraday Soc.* **62**, 2069–2075 (1966).
- Yuster, P. H. & Delbecq, C. J. Some Optical Properties of Potassium Iodide-Thallium Phosphors. *J. Chem. Phys.* **21**, 892–898 (1953).
- Xie, W. & Li, H. Alumina-supported potassium iodide as a heterogeneous catalyst for biodiesel production from soybean oil. *J. Mol. Catal. A: Chem.* **255**, 1–9 (2006).
- Prajapati, D. & Sandhu, J. S. Cadmium iodide as a new catalyst for knoevenagel condensations. *J. Chem. Soc. Perkin Trans. 1*, 739–740 (1993).
- Smanik, P. A. *et al.* Cloning of the human sodium iodide symporter. *Biophys. Res. Commun.* **226**, 339–345 (1996).
- Mao, H. K., Hemley, R. J., Chen, L. C., Shu, J. F. & Finger, L. W. X-ray diffraction to 302 gigapascals: High-pressure crystal structure of cesium iodide. *Science* **246**, 649 (1989).
- Eremets, M. I., Shimizu, K., Kobayashi, T. C. & Amaya, K. Metallic CsI at pressures of up to 220 gigapascals. *Science* **281**, 1333 (1998).
- Hemley, R. J. Superconductivity in a Grain of Salt. *Science* **281**, 1296 (1998).
- Huang, T. L. & Ruoff, A. L. Equation of state and high-pressure phase transition of CsI. *Phys. Rev. B* **29**, 1112 (1984).
- Mao, H. K. *et al.* High-pressure phase transition and equation of state of CsI. *Phys. Rev. Lett.* **64**, 1749 (1990).
- Xu, Y. *et al.* Superconducting high-pressure phase of cesium iodide. *Phys. Rev. B* **79**, 144110 (2009).
- Eremets, M. I., Shimizu, K., Kobayashi, T. C. & Amaya, K. Metallic CsI at pressures of up to 220 gigapascals. *Science* **281**, 1333 (1998).
- Eremets, M. I., Shimizu, K., Kobayashi, T. C. & Amaya, K. Metallization and superconductivity in CsI at pressures up to 220 GPa. *J. Phys. Condens. Matter* **10**, 11519 (1998).
- Zhang, F., Gale, J. D., Uberuaga, B. P., Stanek, C. R. & Marks, N. A. Importance of dispersion in density functional calculations of cesium chloride and its related halides. *Phys. Rev. B* **88**, 054112 (2013).
- De Mico, A., Margarita, R., Parlanti, L., Vescovi, A. & Piancatelli, G. A versatile and highly selective hypervalent iodine (III)/2, 2, 6, 6-tetramethyl-1-piperidinyloxy-mediated oxidation of alcohols to carbonyl compounds. *J. Org. Chem.* **62**, 6974–6977 (1997).
- Wirth, T. Hypervalent iodine chemistry in synthesis: scope and new directions. *Angew. Chem.-Int. Edit.* **44**, 3656–3665 (2005).
- Frigerio, M., Santagostino, M., Sputore, S. & Palmisano, G. Oxidation of Alcohols with *o*-Iodoxybenzoic Acid in DMSO: A New Insight into an Old Hypervalent Iodine Reagent. *J. Org. Chem.* **60**, 7272–7276 (1995).
- Moriarty, R. M. & Vaid, R. K. Carbon-carbon bond formation via hypervalent iodine oxidations. *Synthesis* **6**, 431–447 (1990).
- Richardson, R. D. & Wirth, T. Hypervalent iodine goes catalytic. *Angew. Chem.-Int. Edit.* **45**, 4402–4404 (2006).
- Tohma, H., Takizawa, S., Maegawa, T. & Kita, Y. Facile and clean oxidation of alcohols in water using hypervalent iodine (III) reagents. *Angew. Chem.-Int. Edit.* **39**, 1306–1308 (2000).
- Mooney, R. C. L. The Configuration of the Triiodide Group in Ammonium Triiodide Crystals. *Z. Krist.* **90**, 143 (1935).
- Lewis, G. N. The atom and the molecule. *J. Am. Chem. Soc.* **38**, 762 (1916).
- Bozorth, R. M. & Pauling, L. The crystal structures of cesium Tri-Iodide and cesium Dibromo-Iodide. *J. Am. Chem. Soc.* **47**, 1561–1571 (1925).
- Briggs, T. R. The Polyiodides of Cesium. II. *J. Phys. Chem.* **34**, 2260 (1930).
- Briggs, T. R., Greenawald, J. A. & Leonard, J. W. The Polyiodides of Cesium—Cesium Iodide, Iodine, and Water at 25°. *J. Phys. Chem.* **34**, 1951–1960 (1930).
- Briggs, T. R., Clack, K. D. G., Ballard, K. H. & Sassaman, W. A. Polyiodides of Potassium. II. The Ternary System Potassium Iodide–Iodine–Water. *J. Phys. Chem.* **44**, 350–372 (1940).
- Tasman, H. A. & Boswijk, K. H. Re-investigation of the crystal structure of CsI₃. *Acta Cryst.* **8**, 59–60 (1955).
- Havinga, E. E., Boswijk, K. H. & Wiebenga, E. H. The crystal structure of Cs₂I₈ (CsI₄). *Acta Cryst.* **7**, 487–490 (1954).
- Breneman, G. L. & Willett, R. D. The crystal structure of cesium tribromide and a comparison of the Br₃⁻ and I₃⁻ systems. *Acta Cryst. B* **25**, 1073–1076 (1969).
- Zhang, W. *et al.* Unexpected Stable Stoichiometries of Sodium Chlorides. *Science* **342**, 1502–1505 (2013).
- Wang, Y., Lv, J., Zhu, L. & Ma, Y. CALYPSO: A method for crystal structure prediction. *Comput. Phys. Commun.* **183**, 2063–2070 (2012). CALYPSO Code is Free for Academic Use. Please Register at <http://www.calypso.cn>.
- Wang, Y., Lv, J., Zhu, L. & Ma, Y. Crystal structure prediction via particle-swarm optimization. *Phys. Rev. B* **82**, 094116 (2010).
- Wang, Y. *et al.* An effective structure prediction method for layered materials based on 2D particle swarm optimization algorithm. *J. Chem. Phys.* **137**, 224108 (2012).
- Lv, J., Wang, Y., Zhu, L., & Ma, Y. Particle-swarm structure prediction on clusters. *J. Chem. Phys.* **137**, 084104 (2012).
- Zhang, M. *et al.* Superhard BC₃ in Cubic Diamond Structure. *Phys. Rev. Lett.* **114**, 015502 (2015).
- Zhou, D., Li, Q., Ma, Y., Cui, Q. & Chen, C. Unraveling convoluted structural transitions in SnTe at high pressure. *J. Phys. Chem. C* **117**, 5352 (2013).
- Peng, F., Miao, M., Wang, H., Li, Q. & Ma, Y. Predicted lithium-boron compounds under high pressure. *J. Am. Chem. Soc.* **134**, 18599 (2012).

39. Wang, H., John, S. T., Tanaka, K., Iitaka, T. & Ma, Y. Superconductive sodalite-like clathrate calcium hydride at high pressures. *Proc. Natl. Acad. Sci. USA* **109**, 6463 (2012).
40. Zhu, L. *et al.* Spiral chain O₄ form of dense oxygen. *Proc. Natl. Acad. Sci. USA* **109**, 751 (2012).
41. Li, Q., Zhou, D., Zheng, W., Ma, Y. & Chen, C. Global structural optimization of tungsten borides. *Phys. Rev. Lett.* **110**, 136403 (2013).
42. Lu, C., Miao, M. & Ma, Y. Structural Evolution of Carbon Dioxide under High Pressure. *J. Am. Chem. Soc.* **135**, 14167 (2013).
43. Li, Q. *et al.* A novel low compressible and superhard carbon nitride: Body-centered tetragonal CN₂. *Phys. Chem. Chem. Phys.* **14**, 13081 (2012).
44. Lu, S., Wang, Y., Liu, H., Miao, M. S. & Ma, Y. Self-assembled ultrathin nanotubes on diamond (100) surface. *Nature Commun.* **5**, 3666 (2014).
45. Zhu, L., Liu, H., Pickard, C. J., Zou, G. & Ma, Y. Reactions of xenon with iron and nickel are predicted in the Earth's inner core. *Nature Chem.* **6**, 644–648 (2014).
46. Wei, S. *et al.* High-pressure phase transition of cesium chloride and cesium bromide. *Phys. Chem. Chem. Phys.* **16**, 17924–17929 (2014).
47. Hach, R. J. & Rundle, R. E. The Structure of Tetramethylammonium Pentaiodide1, 1a. *J. Am. Chem. Soc.* **73**, 4321 (1951).
48. Rundle, R. E. On the Problem Structure of XeF₄ and XeF₂. *J. Am. Chem. Soc.* **85**, 112 (1963).
49. Pimentel, G. C. The bonding of trihalide and bifluoride ions by the molecular orbital method. *J. Chem. Phys.* **19**, 446 (1951).
50. Kresse, G. & Furthmüller, J. Efficient iterative schemes for *ab initio* total-energy calculations using a plane-wave basis set. *Phys. Rev. B* **54**, 11169 (1996).
51. Perdew, J. P., Burke, K. & Ernzerhof, M. Generalized gradient approximation made simple. *Phys. Rev. Lett.* **77**, 3865 (1996).
52. Blöchl, P. E. Projector augmented-wave method. *Phys. Rev. B* **50**, 17953–17979 (1994).
53. Togo, A., Oba, F. & Tanaka, I. First-principles calculations of the ferroelastic transition between rutile-type and CaCl₂-type SiO₂ at high pressures. *Phys. Rev. B* **78**, 134106 (2008).
54. Bader, R. F. W. *Atoms in Molecules: A Quantum Theory*, Oxford Univ. Press, (1990).
55. Baroni, S., Giannozzi, P. & Testa, A. Green's-function approach to linear response in solids. *Phys. Rev. Lett.* **58**, 1861 (1987).
56. Giannozzi, P., De Gironcoli, S., Pavone, P. & Baroni, S. *Ab initio* calculation of phonon dispersions in semiconductors. *Phys. Rev. B* **43**, 7231 (1991).
57. Giannozzi, P. *et al.* QUANTUM ESPRESSO: a modular and open-source software project for quantum simulations of materials. *J. Phys. Condens. Matter* **21**, 395502 (2009).
58. Pauling, L. *The Nature of the Chemical Bond*, 2nd ed. Cornell Univ. Press, Ithaca, NY, p111 (1948).
59. Cartmell, E. & Fowles, G. W. A. Valency and Molecular Structure. *Butterworth and Co. Ltd.*, London, p177 (1956).
60. Musher, J. I. The chemistry of hypervalent molecules. *Angew. Chem. Int. Ed. Engl.* **8**, 54–68 (1969).
61. Allen, P. B. Neutron spectroscopy of superconductors. *Phys. Rev. B* **6**, 2577 (1972).
62. Allen, P. B. & Dynes, R. C. Transition temperature of strong-coupled superconductors reanalyzed. *Phys. Rev. B* **12**, 905 (1975).

Acknowledgements

This work is supported by the China 973 Program (2011CB808200), the Natural Science Foundation of China under 51202084, 11474125, and 11274136, the 2012 Changjiang Scholars Program of China, Changjiang Scholar and Innovative Research Team in University (IRT1132), Project 2015129 Supported by Graduate Innovation Fund of Jilin University. Parts of the calculations were performed in the High Performance Computing Center (HPCC) of Jilin University.

Author Contributions

Q.L. conceived and provided critical ideas for the work. S.W. performed most of the calculations. S.W., J.W., S.D. and S.Z. analysed the data. J.W. carried out the phonon calculations. All authors commented on the manuscript. S.W. and Q.L. wrote the paper.

Additional Information

Competing financial interests: The authors declare no competing financial interests.

How to cite this article: Wei, S. *et al.* Hypervalent Iodine with Linear Chain at High Pressure. *Sci. Rep.* **5**, 14393; doi: 10.1038/srep14393 (2015).



This work is licensed under a Creative Commons Attribution 4.0 International License. The images or other third party material in this article are included in the article's Creative Commons license, unless indicated otherwise in the credit line; if the material is not included under the Creative Commons license, users will need to obtain permission from the license holder to reproduce the material. To view a copy of this license, visit <http://creativecommons.org/licenses/by/4.0/>